



Self-Propagating High-Temperature Synthesis
Самораспространяющийся высокотемпературный синтез



UDC 621.762

<https://doi.org/10.17073/1997-308X-2023-1-28-38>

Research article

Научная статья



Formation of products upon ignition, combustion and melting of mixtures of high-entropy alloy FeNiCoCrCu with titanium and carbon

S. G. Vadchenko[✉], Yu. S. Vergunova, A. S. Rogachev,
I. D. Kovalev, N. I. Mukhina

Merzhanov Institute of Structural Macrokinetics and Materials Science of the Russian Academy of Sciences
8 Akademian Osip'yan Str., Chernogolovka, Moscow region 142432, Russian Federation

✉ vadchenko@ism.ac.ru

Abstract. The dependence of the ignition temperature, combustion rate and composition of the resulting products on the concentration of Ti + C in mixtures with powder of a high-entropy alloy (HEA) FeNiCoCrCu and the initial mixture of metals forming it (MIX) has been studied. HEA was obtained by mechanical activation (MA) of a mixture of metal powders in argon. At the melting temperature, the high-entropy FeNiCoCrCu alloy decomposes into several phases, but the basis of the HEA alloy, as well as the alloy obtained by melting and crystallizing MIX, is a 5-component phase with an average formula $\text{Cu}_{1.2}\text{Fe}_{1.4}\text{Ni}_{1.4}\text{Co}_{1.4}\text{Cr}$. In addition, 5, 4, and 3-component phases with averaged formulas $\text{Cu}_2\text{Ni}_2\text{Co}_2\text{Fe}_2\text{Cr}$, $\text{Cu}_3\text{Ni}_3\text{Co}_{2.9}\text{Fe}_{2.5}\text{Cr}$, $\text{Cu}_{4.8}\text{Ni}_{4.5}\text{Co}_{4.6}\text{Fe}_{4.2}\text{Cr}$, $\text{Cu}_{40}\text{Fe}_2\text{Ni}_4\text{Co}_2\text{C}$, $\text{Cr}_{12.5}\text{Fe}_{3.2}\text{Co}_{2.6}\text{Ni}$ and $\text{Co}_{3.2}\text{Fe}_{3.5}\text{Cr}$ are present in small amounts in the binder. Experiments on the ignition and combustion of mixtures of MIX and HEA with Ti + C were carried out in argon at atmospheric pressure. The combustion rate, ignition temperature, and maximum temperature reached in the thermal explosion of MIX and HEA mixtures with Ti + C increase with increasing Ti + C concentration. Due to the low exothermicity of the mixtures, the experiments were carried out at an initial temperature of 500 °C. At this initial temperature, the combustion limit of the samples occurs when the Ti + C concentration in the HEA and MIX mixtures is less than 30 %. Based on the results of scanning electron microscopy, the volume concentration of the number of titanium carbide (TiC) particles in molten samples was calculated. In an alloy with a HEA binder, the number of TiC particles per unit volume is 1.5–3.0 times greater than in an alloy with a MIX binder, and their size is correspondingly smaller. With an increase in the concentration of Ti + C from 30 to 40 % in a mixture with HEA, the number of TiC particles per unit volume decreases. In a mixture with MIX, the number of TiC particles per unit volume passes through a minimum. This is due to two opposite processes: on the one hand, the probability of the generation of TiC particles increases, on the other hand, their coagulation occurs.

Keywords: high-entropy alloys, mechanical activation, cermets, titanium carbide, ignition, combustion, melting, energy-releasing additive Ti + C

Acknowledgements: the work was carried out at the expense of a grant from the Russian Science Foundation (Project No. 20-13-00277).

For citation: Vadchenko S.G., Vergunova Yu.S., Rogachev A.S., Kovalev I.D., Mukhina N.I. Formation of products upon ignition, combustion and melting of mixtures of high-entropy alloy FeNiCoCrCu with titanium and carbon. *Powder Metallurgy and Functional Coatings*. 2023;17(1):28–38. <https://doi.org/10.17073/1997-308X-2023-1-28-38>

Формирование продуктов при воспламенении, горении и плавлении смесей высокоэнтروпийного сплава FeNiCoCrCu с титаном и углеродом

С. Г. Вадченко[✉], Ю. С. Вергунова, А. С. Рогачев,
И. Д. Ковалев, Н. И. Мухина

Институт структурной макрокинетики и проблем материаловедения им. А.Г. Мержанова РАН
Россия, 142432, Московская обл., г. Черноголовка, ул. Академика Осипьяна, 8

✉ vadchenko@ism.ac.ru

Аннотация. Исследована зависимость температуры воспламенения, скорости горения и состава формирующихся продуктов от концентрации Ti + C в смесях с порошком высокоэнтропийного сплава (ВЭС) FeNiCoCrCu и исходной смесью образующих его металлов (MIX). ВЭС получали методом механической активации (МА) смеси порошков металлов в среде аргона. При температуре плавления высокоэнтропийный сплав FeNiCoCrCu распадается на несколько фаз, но основу этого ВЭС, а также сплава, полученного при плавлении и кристаллизации MIX, составляет 5-компонентная фаза с усредненной формулой $\text{Cu}_{1,2}\text{Fe}_{1,4}\text{Ni}_{1,4}\text{Co}_{1,4}\text{Cr}$. Кроме того, в небольших количествах в связке присутствуют 5-, 4- и 3-компонентные фазы с усредненными формулами $\text{Cu}_2\text{Ni}_2\text{Co}_2\text{Fe}_2\text{Cr}$, $\text{Cu}_3\text{Ni}_3\text{Co}_{2,9}\text{Fe}_{2,5}\text{Cr}$, $\text{Cu}_{4,8}\text{Ni}_{4,5}\text{Co}_{4,6}\text{Fe}_{4,2}\text{Cr}$, $\text{Cu}_{40}\text{Fe}_2\text{Ni}_4\text{Co}_2\text{C}$, $\text{Cr}_{12,5}\text{Fe}_{3,2}\text{Co}_{2,6}\text{Ni}$ и $\text{Co}_{3,2}\text{Fe}_{3,5}\text{Cr}$. Эксперименты по воспламенению и горению смесей MIX и ВЭС с Ti + C проводили в аргоне при атмосферном давлении. Скорость горения, температура воспламенения и максимальная температура, достигаемая при тепловом взрыве смесей MIX и ВЭС с Ti + C, растут с увеличением концентрации Ti + C. Из-за малой экзотермичности смесей эксперименты проводили при начальной температуре 500 °C – в этом случае предел горения образцов наступает при концентрации Ti + C в смесях ВЭС и MIX <30 %. По результатам сканирующей электронной микроскопии рассчитана объемная концентрация частиц карбида титана (TiC) в расплавленных образцах. В сплаве со связкой из ВЭС количество частиц TiC в единице объема в 1,5–3,0 раза больше, чем в сплаве со связкой из MIX, а их размер соответственно меньше. С повышением концентрации Ti + C от 30 до 40 % в смеси с ВЭС количество числа частиц TiC в единице объема уменьшается. В смеси с MIX объемная концентрация частиц TiC проходит через минимум. Это связано с двумя противоположными процессами – с одной стороны, увеличивается вероятность зарождения частиц TiC, а с другой – происходит их коагуляция.

Ключевые слова: высокоэнтропийные сплавы, механическая активация, керметы, карбид титана, воспламенение, горение, плавление, энерговыделяющая добавка Ti + C

Благодарности: работа выполнена за счет гранта Российского научного фонда (проект № 20-13-00277).

Для цитирования: Вадченко С.Г., Вергунова Ю.С., Рогачев А.С., Ковалев И.Д., Мухина Н.И. Формирование продуктов при воспламенении, горении и плавлении смесей высокоэнтропийного сплава FeNiCoCrCu с титаном и углеродом. *Известия вузов. Порошковая металлургия и функциональные покрытия*. 2023;17(1):28–38.
<https://doi.org/10.17073/1997-308X-2023-1-28-38>

Introduction

High-entropy alloys (HEAs) are a new class of metallic compounds consisting of at least 5 major elements whose concentration varies between 5 and 35 at.%. HEAs generally demonstrate the formation of a simple solid solution structure – VCC, FCC, HCP, or their combinations – instead of intermetallic phases stabilized due to the high configuration entropy of their mixing [1; 2]. Due to the alloys structure peculiarities, they can be used to create new materials with unique properties [3–9].

Recently, HEAs have been considered as a new metallic binder to improve the HEA-based materials performance properties:

- WC–CoCrFeNiMn [10],
- SiC–CoCrFeMnNi [11],
- TiC–FeCrNiCoAlCu [12; 13],
- TiC–FeMnCrNiCo [14],
- TiCN–AlCoCrFeNi [15],
- TiCN–CoCrFeNiCu [16],
- Ti(C,N)–HEA based on (Co, Fe, Ni) [17],
- TiCN–CrMnFeCoNi [18],
- TiC–CoCrFeNiMe (Me = Mn, Ti, Al) [19].

The work [13] showed that the FeCoCrAlCu HEA-based coatings reinforced with TiC (50 %) obtained by laser surface doping (LSD) have a maximum microhardness of 10.82 GPa, whereas without the reinforcing additive the microhardness was 6.29 GPa. In addition, the TiC inclusions located along the grain boundaries of the HEA prevented their growth and improved the wear resistance. In particular, for the FeCoCrAlCu + 50 % TiC composite coating, the microhardness, wear volume and specific wear rate were 10.78 GPa, $5.2 \cdot 10^{-5} \mu\text{m}^3$ and $9.6 \cdot 10^{-5} \text{mm}^3/(\text{N} \cdot \text{m})$, respectively.

The authors [16] investigated the mechanical activation effect (MA) on the resulting CoCrFeNiCu HEA-powder properties used as a binder in the Ti(C,N) cermets manufacturing by vacuum sintering. The CoCrFeNiCu HEA-powders were obtained by mechanical fusion in a planetary ball mill. With increasing grinding time (τ_{MA}), the diffraction peaks gradually broaden and their intensities decrease. The face-centered cubic (FCC) phase (111) formation with lattice parameter $a = 3.537 \text{ \AA}$ and the secondary volume-centered cubic (VCC) phase (110) release at $a = 2.905 \text{ \AA}$ occurred after $\tau_{\text{MA}} = 90 \text{ h}$, and a diffraction peaks slight broadening was observed when τ_{MA}

was increased to 120 h. In the work [16], MA HEA-powders were mixed with $\text{Ti}(\text{C}_{0.7}\text{N}_{0.3})$ (1.2 μm), WC (2.3 μm), Mo_2C (1.75 μm), TaC (1.25 μm) in a ball mill at $v = 56$ rpm and $\tau_{\text{MA}} = 72$ h. Despite this two-stage long MA time, the authors [16] conclude that the CoCrFeNiCu HEA is a good variant to use as a new binder in Ti(C,N) based cermets as it has higher fracture strength (8.8 $\text{MPa} \cdot \text{m}^{-1/2}$) and hardness (1726 HV) compared to conventional nickel-based cermets.

The other authors [17] also used the same methodology: the formation of a single-phase solid solution with a FCC structure and lattice parameter 0.3601 Å of composition CoCrCuFeNi occurred during $\tau_{\text{MA}} = 10$ h.

Despite the MA method frequent use for obtaining alloys, its disadvantages are: the long preparation time (10–120 h) and small amounts of obtained materials. At the same time, in the work [20], a single-phase solid solution with an FCC structure and the lattice parameter 3.597 Å with a uniform distribution of all elements was already obtained at $\tau_{\text{MA}} = 120$ min.

Earlier [19] the possibility of obtaining cermet based on a high-entropic binder (CoCrFeNiMn, CoCrFeNiTi and CoCrFeNiAl) and an additive mixture of Ti + C by self-propagating high-temperature synthesis (SHS), which is realized due to heat released during the titanium with carbon exothermic reaction, was investigated. In the combustion wave the melting of 5 elements occurs with the multicomponent melt CoCrFeNiMe ($Me = \text{Mn, Ti, Al}$) formation, which is crystallized in the HEA as a binding phase. The combustion rate and temperature gradually decrease with increasing amount of binder. According to scanning electron microscopy (SEM) and energy dispersive spectroscopy (EDXA) results, all synthesized materials consist of TiC grains and a two-phase (FCC and VCC) metal binder. The Vickers microhardness of the pressed metal-ceramic materials with 30 % binder is in the range of 10–17 GPa, rising with the VCC to FCC ratio increase.

The present work studies for the first time the possibility of obtaining TiC–FeNiCoCrCu cermets with different contents of high-entropic FeNiCoCrCu binder by SHS. The dependence of the ignition temperature, combustion rate and composition of the products formed on the concentration of Ti + C in mixtures with FeNiCoCrCu HEA powder and the initial mixture of the metals forming them was investigated.

Materials and methodology

Titanium powders (PTS-1, 99.6 %, average particle size $d = 50$ μm , production of JSC “Polema”, Tula) and carbon (P803, $d = 0.1$ μm , production of LLC PCC “Ekopolza”, Astrakhan) in equiatomic ratio were mixed

in a porcelain mortar to get a homogeneous mass. Also prepared the equiatomic mixture of iron (R-10, 99.96 %, $d = 10 \div 20$ μm , JSC “Polema”, Tula), nickel (PNE-1, 99.5 %, $d = 45 \div 60$ μm , LLC PME “Ural Atomization”, Chelyabinsk), cobalt (PC1-U, 99.7 %, $d = 71$ μm , CCM “Ekotek”, Moscow), chromium (PKh1, TU 14-1-1474-75, $d < 125$ μm , MC “Atom”, Ekaterinburg) and copper (PMS-1, $d = 45 \div 100$ μm , LLC PME “Ural Atomization”, Chelyabinsk). All metals of this MIX mixture (Fe + Ni + Co + Cr + Cu) retained their individuality.

Part of this mixture MIX was subjected to mechanical activation in a planetary mill Activator 2S (CJSC “Activator”, Novosibirsk). The processing was carried out in steel drums in an argon atmosphere at a pressure of 4 bar. The ratio of the mixture mass to the balls mass was 1:20, the drums rotational speed was 694 min^{-1} , the processing time – 120 min. As a result, the MA produced particles consisting of the FeNiCoCrCu HEA, which is a solid solution with a face-centered cubic lattice. The particle size distribution was studied with a laser particle analyzer “Microsizer-201C” (VA Instalt, St. Petersburg). Grinding and polishing samples were carried out according to the standard method on a DP-U4 (Struers, Denmark) grinding and polishing machine. Scanning electron microscopy (SEM) was performed on a LEO 1450 VP microscope (Carl-Zeiss SMT AG, Germany). X-ray phase analysis (XRD) was performed on diffractometer DRON-3 (Scientific and Production Enterprise “Burevestnik”, St. Petersburg) on FeK_α radiation. MIX and HEA powders were sintered by the spark plasma sintering (SPI) method in a vacuum in the “Labox 650 facility” installation (Sinter Land, Japan) at a load of 50 MPa for 20 min. Microhardness of samples was measured on installation PMT-3 (LOMO, St. Petersburg).

Previously prepared mixtures in the ratio $x(\text{Ti} + \text{C})$ and $(100 - x)\text{MIX}$, where $x = 10, 20, 30, 40, 50, 60, 70, 80$ and 90 %, were again mixed in a porcelain mortar until a homogeneous mass was obtained. To obtain relatively homogeneous samples from mixtures of Ti + C with HEA particles with a ratio of $x(\text{Ti} + \text{C})$ to $(100 - x)$ HEA, where $x = 30, 40, 50, 60$ and 70 %, pellets containing 2 to 5 HEA particles surrounded by Ti + C mixture were made using a 2 % butyral resin solution in alcohol. It is difficult to obtain homogeneous mixtures with more Ti + C mixture due to the large difference in the HEAs and titanium particles sizes (Fig. 1).

To study the obtained mixtures ignition parameters the samples with diameter $D = 3$ and 5 mm and height up to $1D$ were pressed. The scheme of the experiments to determine the ignition temperature is shown in Fig. 2, a [21]. Cylindrical samples were placed on a flat thermocouple 30 μm thick in a crucible made of boron nitride or graphite. The crucible rested on a graphite

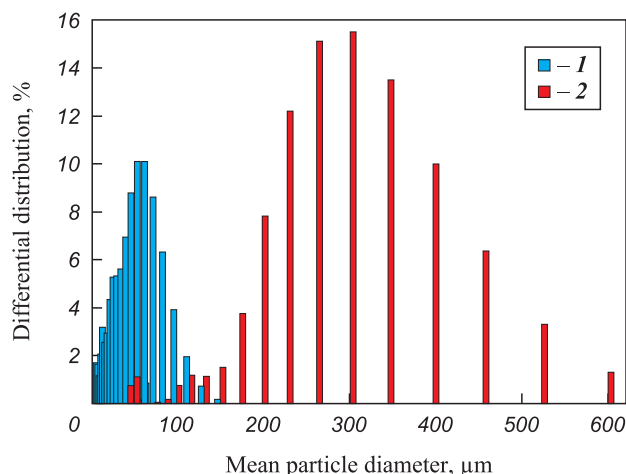


Fig. 1. Titanium (1) and HEA (2) particle size distribution histogram

Рис. 1. Гистограмма распределения по размерам частиц титана (1) и ВЭС (2)

strip heated by an electric current to the sample ignition or melting temperature.

To study combustion, the samples were pressed in the form of 6×30 mm plates with a thickness of 2.5–3.0 mm. The relative density of the samples was 0.45–0.5. They were placed between two graphite blocks with heaters

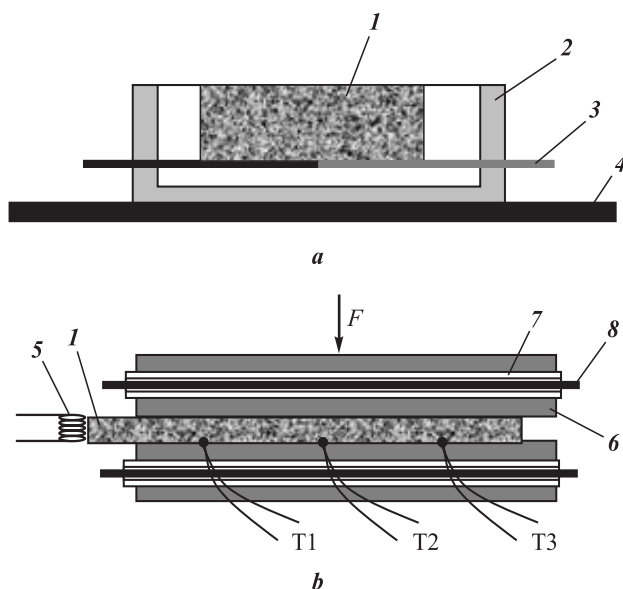


Fig. 2. Samples (a) and the combustion rate (b) measuring the ignition temperature schemes

1 – sample, 2 – crucible, 3 – thermocouple, 4 – graphite heater strip, 5 – initiating coil, 6 – graphite plate with heaters, 7 – Al_2O_3 tubes, 8 – heater, F – load, T1–T3 – thermocouples

Рис. 2. Схемы измерения температуры воспламенения образцов (a) и скорости горения (b)

1 – образец, 2 – тигель, 3 – термопара, 4 – графитовый ленточный нагреватель, 5 – инициирующая спираль, 6 – графитовая пластина с нагревателями, 7 – трубки из Al_2O_3 , 8 – нагреватель, F – нагрузка, T1–T3 – термопары

inside. Combustion was initiated by a coil heated by an electric current. The samples combustion rate was determined as the ratio of the distance between the thermocouples T1–T2–T3 to the time of the combustion wave passing between them. The experiments were performed in argon at atmospheric pressure.

Results and discussion

Ignition

Figure 3 shows characteristic thermograms of the ignition of samples pressed from the initial powders at different concentrations in the mixture Ti + C. The Ti + C mixture samples ignition temperature is about 1200 °C. When the concentration of Ti + C is reduced to 80 %, the metal mixtures ignition temperature is $t = 1080 \pm 30$ °C. The lowering of the ignition temperature of mixtures containing copper may be due to its melting ($t_m = 1083$ °C). The copper melting increases its volume by 6 vol.% [22], which leads to better contacts between the particles, and also starts the reaction of titanium with copper, which, despite the weak exothermicity (calculated values of formation CuTi enthalpy – 79 kJ/mol [23]), can initiate the titanium with carbon interaction.

The ignition temperatures of samples from mixtures based on HEA-powders at the Ti + C concentration in the mixture equal to 30–70 % are close to the ignition temperature of the initial mixture Ti + C, since due to the large size of HEA-particles they play the role of an inert diluent.

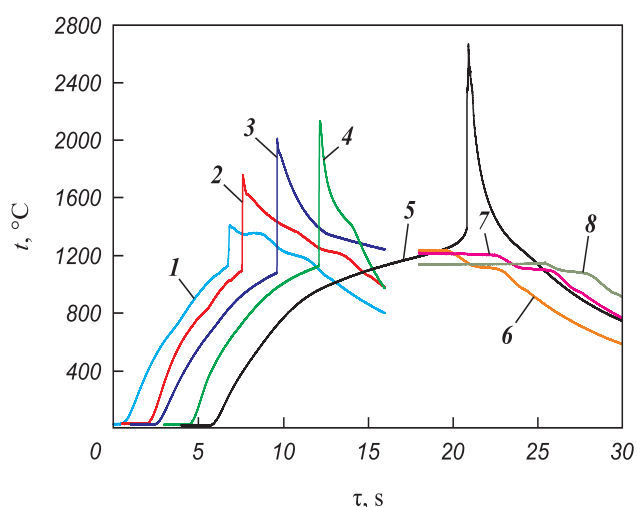


Fig. 3. Initial mixtures (Ti + C) + MIX ignition (1–5) and cooling (6–8) thermograms characteristic view Ti + C, %: 30 (1), 40 (2), 60 (3), 80 (4), 100 (5), 20 (6–8)

Рис. 3. Характерный вид термограмм воспламенения (1–5) и охлаждения (6–8) исходных смесей (Ti + C) + MIX Ti + C, %: 30 (1), 40 (2), 60 (3), 80 (4), 100 (5), 20 (6–8)

When cooling the compositions ignition products with Ti + C concentration equal to 30–40 %, two inflections (plateaus) around 1360 and 1200 °C are observed in the thermograms associated with crystallization of the melt of polymetallic binder. The temperature of the first plateau is close to the temperature of endothermic peaks observed in differential scanning calorimetry (DSC) Fe + Ni + Co + Cr + Cu (1359 °C) mixture and FeNiCoCrCu (1365 °C) HEA in the work [20], and caused in the first case, apparently, the resulting compound melting. At Ti + C higher contents, the used method does not allow to register this effect. At the Ti + C content of 10–20 % in the mixture, a plateau near 1200 °C (Fig. 3, curves 6–8) and an inflection near 1100 °C are also observed during cooling.

Combustion

During the samples combustion, size and density practically did not change, since they were under load (compression pressure $F = 0.1$ MPa). Figure 4 shows the combustion products surface structure. Large pores up to 0.5 mm in the sample 0.4(Ti + C) + 0.6HEA were formed as a result of HEA-particles melting and TiC framework melt spreading.

The initial samples density, calculated as the measured mass to the geometric volume ratio is shown in Table 1. Since the experiments were carried out under load, the samples size changes after combustion were insignificant.

Combustion thermograms characteristic view is shown in Fig. 5. Since at less than 60 % Ti + C in the

mixture at room temperature the samples did not burn or burn unstably, all experiments were conducted at an initial temperature of 500 ± 10 °C. Samples with [Ti + C] concentrations ≤ 30 % did not burn at this initial temperature.

Figure 6 shows the dependence on the Ti + C concentration of the mixtures with MIX and HEA combustion rate and the mixtures Ti + C and MIX difference $\Delta t = t_{\max} - t_{\text{ig}}$ between the maximum temperature reached at ignition and the ignition temperature. At a small difference Δt , the self-propagating combustion mode is not realized in this system.

The main contribution to heat release during mixtures ignition and combustion is made by the titanium carbide formation reaction. Titanium can also react with the heat emission with all metals included in the HEA-mixture, and chromium can interact with carbon to form carbide Cr_3C_2 . The formation enthalpy of all these compounds is much less than for the Ti + C reaction, and these compounds are not detected on the X-rays. But the reaction mechanisms of composite formation when using MIX and HEA as a binder are different, which is due to the difference in the Ti + C mixtures structure. In the former case, the contact surface between titanium and carbon particles is much smaller because the unit cell of the mixture consists of metal particles and carbon distributed between them. Assuming that the metal particles are close in size, then per titanium particle in the cell, depending on Ti + C concentration, there are approximately from 1 (when $x = 90$ % Ti + C) to 20

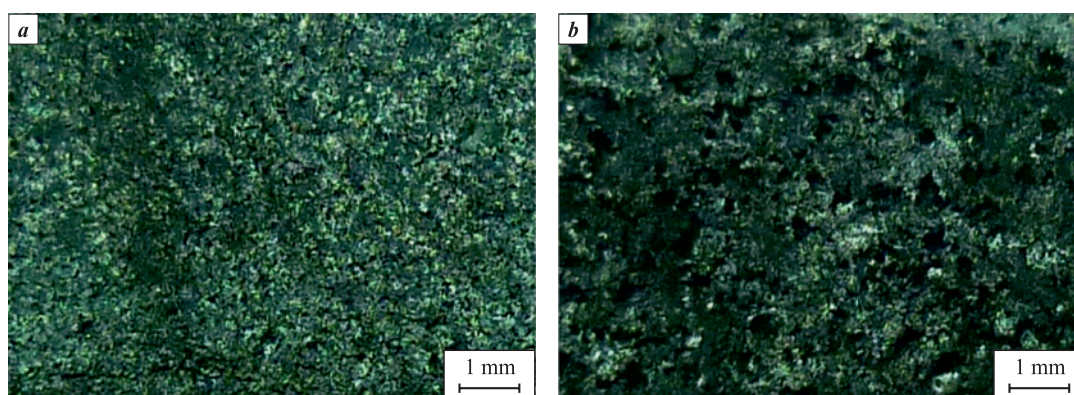


Fig. 4. 0.4(Ti + C) + 0.6MIX (a) and 0.4(Ti + C) + 0.6HEA (b) mixtures combustion products surface structure

Рис. 4. Структура поверхности продуктов горения смесей 0,4(Ti + C) + 0,6MIX (a) и 0,4(Ti + C) + 0,6ВЭС (b)

Table 1. Samples density, g/cm³, from Ti + C with MIX and HEA mixtures

Таблица 1. Плотность образцов, г/см³, из смесей Ti + C с MIX и ВЭС

Binder composition	Ti + C, %							
	30	40	50	60	70	80	90	100
MIX	3.23	3.02	2.51	2.51	2.50	2.04	1.88	1.85
HEA	3.20	3.01	2.79	2.78	2.48	—	—	1.85

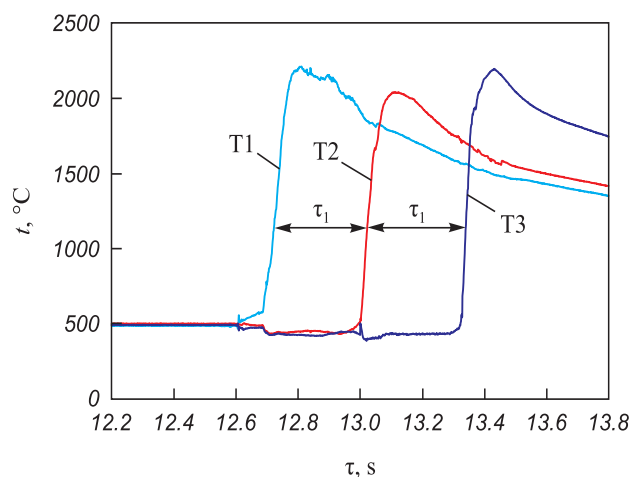


Fig. 5. Mixture 70(Ti + C) + 30MIX sample combustion thermogram

Рис. 5. Термограмма горения образца из смеси 70(Ti + C) + 30MIX

(when $x = 10\%$ Ti + C) particles of other metals. In the latter case, the titanium particle is surrounded by a small portion of carbon, i.e., the Ti + C mixture appears diluted in both thermal and concentration (Ti/C) terms. As the Ti + C concentration decreases, the mechanism of propagation of the combustion wave changes from frontal to percolation. The HEA-powder particles case whose are several times larger than those of the parent metals, only thermal dilution takes place, and the transition from the frontal to percolation combustion mechanism occurs at lower Ti + C concentrations [24].

Figure 7 shows the combustion products change in the phase composition from FeNiCoCrCu to TiC alloys when the Ti + C concentration in the mixture increases from 0 to 100 %.

Mixtures ignition and melting products

At high concentrations in titanium and carbon mixtures high temperatures developed during the samples ignition and combustion, leading to melting of the high-entropic binder or mixture of metals forming it and carbide grains formation. To compare the changes occurring in the MIX and HEA metal mixture binder structure, the powders were heated to the melting temperature. Figure 8 shows characteristic heating and cooling thermograms.

When a metals Fe + Ni + Co + Cr + Cu and HEA mixture is heated to the melting temperature and subsequently crystallized, several plateaus appear on the thermograms. The plateau at heating near 1100 °C occurs due to copper melting. Endothermic peak at close temperatures was observed at DSC of this mixture (1083 °C) and the alloy (1115 °C) in work [20]. Endothermic peaks associated with the melting of the

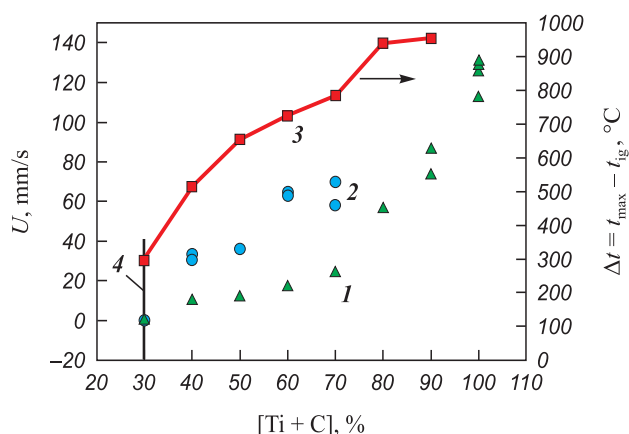


Fig. 6. Dependence of the combustion rate on the concentration of Ti + C in mixtures with MIX (1) and with HPS (2) 3 – difference between the maximum temperature reached at ignition and the ignition temperature 4 – combustion limit

Рис. 6. Зависимость скорости горения от концентрации Ti + C в смесях с MIX (1) и с ВЭС (2) 3 – разность между максимальной температурой, достигаемой при воспламенении, и температурой воспламенения 4 – предел горения

whole composition – metal mixture (1359 °C) and the alloy (1365 °C) – were also observed there.

When cooling the samples after melting the first plateau appears at about 1200 °C and is associated with the crystallization of a more refractory phase – apparently, the main 5-component high-entropic phase. The second plateau at about 1000 °C is due to copper-enriched phase crystallization.

While melting the samples pressed from MIX and HEA powders, several phases are released from the melt (Fig. 9). The basis of the molten MIX and HEA samples is a 5-component phase with the averaged formula of $\text{Cu}_{1.2}\text{Fe}_{1.4}\text{Ni}_{1.4}\text{Co}_{1.4}\text{Cr}$. In addition, the 5-component phases $\text{Cu}_2\text{Ni}_2\text{Co}_2\text{Fe}_2\text{Cr}$, $\text{Cu}_3\text{Ni}_3\text{Co}_{2.9}\text{Fe}_{2.5}\text{Cr}$, $\text{Cu}_{4.8}\text{Ni}_{4.5}\text{Co}_{4.6}\text{Fe}_{4.2}\text{Cr}$, $\text{Cu}_{40}\text{Fe}_2\text{Ni}_4\text{Co}_2\text{Cr}$, $\text{Cu}_{40}\text{Fe}_2\text{Ni}_4\text{Co}_2\text{Cr}$, 4-component with the averaged formula $\text{Cr}_{12.5}\text{Fe}_{3.2}\text{Co}_{2.6}\text{Ni}$, and 3-component with the averaged formula $\text{Co}_{3.2}\text{Fe}_{3.5}\text{Cr}$. During MIX and HEA melting, as well as during ignition and combustion of their mixtures with Ti + C, some of the copper evaporates and precipitates on the sight glass and cold reactor parts.

It is possible that the MIX and HEA melts (Fig. 9) represent the same FCC solid solution but not quite homogeneous in its chemical composition. Part of the chromium is consumed to form ternary and quaternary phases with high chromium concentration, containing no copper and crystallizing in the form of hexagonal tubes filled with the main phase. Concentrations of phases enriched with copper (Fig. 9, 1a, 2a) or chromium (Fig. 9, 1b, 2b) are relatively low and do not show up on the X-ray diffraction patterns (Fig. 10, diffractograms 1, 2). Figure 10 also

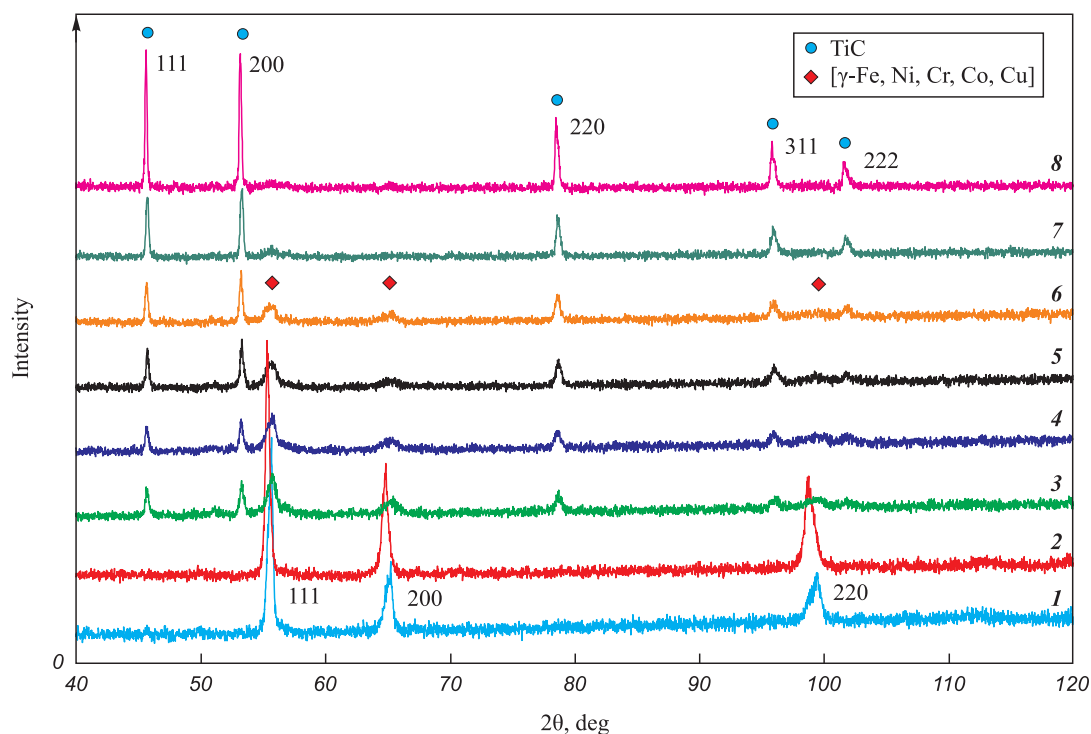


Fig. 7. Mixtures melting products (1, 2) and combustion products (3–8) X-ray patterns
1 – MIX, 2 – HEA, 3 – 40TiC–60MIX, 4 – 40TiC–60HEA, 5 – 60TiC–40MIX, 6 – 60TiC–40HEA, 7 – 80TiC–20MIX, 8 – TiC

Рис. 7. Рентгенограммы продуктов плавления (1, 2) и горения (3–8) смесей
1 – MIX, 2 – ВЭС, 3 – 40TiC–60MIX, 4 – 40TiC–60ВЭС, 5 – 60TiC–40MIX, 6 – 60TiC–40ВЭС, 7 – 80TiC–20MIX, 8 – TiC

shows X-ray diffraction patterns of products obtained by sintering using the SPS method [19]. The peaks shift to the left on the samples X-ray patterns after the MIX and HEA powders melting, as compared to the sintered samples. The chemical composition heterogeneity is evident during sintering at $t = 800$ and 900 °C. At these temperatures the second phase emerges and the peaks split (Fig. 10, diffractograms 3, 4). Both phases formed have a FCC structure. At sintering temperature of 1000 °C composition homogenization occurs.

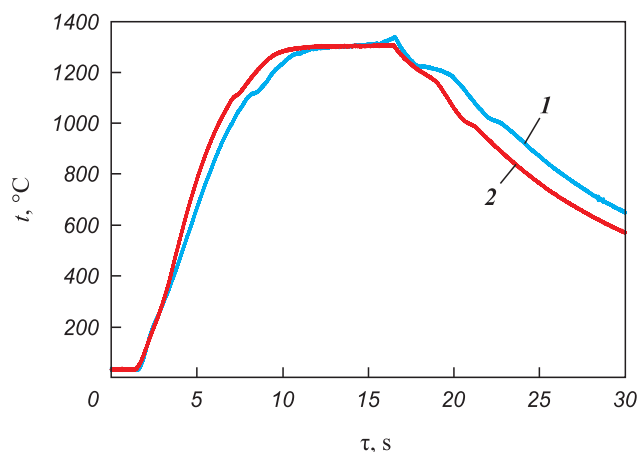


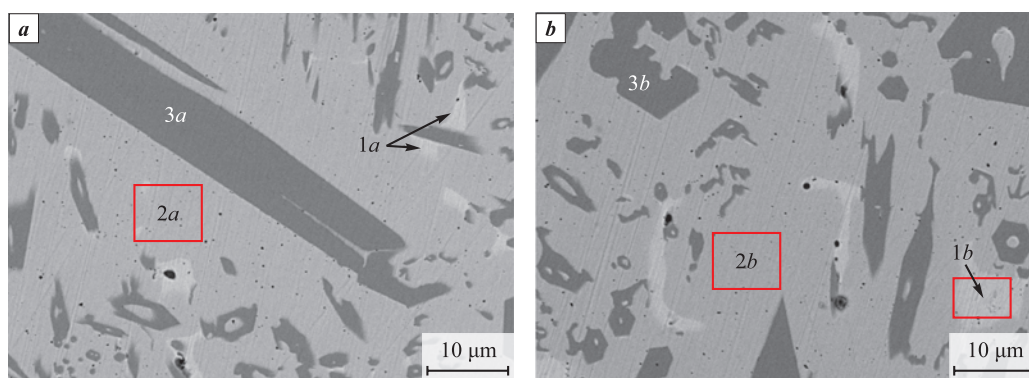
Fig. 8. MIX (1) and HEA (2) heating thermograms

Рис. 8. Термограммы нагрева MIX (1) и ВЭС (2)

Figure 11 shows photographs of microstructures formed during melt crystallization as a result of Ti + C mixtures with MIX and HEA reactions. The dark particles are titanium carbide (TiC). The binder is heterogeneous and includes the same constituents that are released during HEA or MIX melting.

The results of counting the TiC particles number (n) in the molten samples were carried out on the area of the polished section $S = 2,500 \div 10,500 \mu\text{m}^2$ and the volume concentration of particles was calculated by the formula $N = (n/S)^{3/2}$. Table 2 shows the average values from the results of measurements on several polished sections. In the HEA-bonded alloy the number of titanium carbide particles per unit volume was 1.5–3.0 times higher than in the MIX-bonded alloy, and the particle size was correspondingly smaller. As the Ti + C concentration increases from 30 to 40 % in the mixture with HEA, the number of titanium carbide particles per unit volume decreases. In the mixture with MIX the number of particles per unit volume passes through the minimum. This may be due to two processes – on the one hand, the particles nucleation probability increases, and on the other hand, titanium carbide particles coagulation occurs.

Figure 11 also shows that as the concentration of titanium carbide increases, the size of the phases that make up the bond decreases. The basis of the binder, as in the case of the molten MIX and HEA samples,



Range	Cr	Fe	Co	Ni	Cu
1a	2.4	8.4	7.7	9.9	71.5
2a	12.4	23.8	24.9	20.5	18.3
3a	80.1	11.3	8.6	—	—
1b	1.4	4.1	3.5	6.5	84.6
2b	14.8	21.2	22.5	21.5	20.0
3b	78.4	11.2	7.8	2.6	—

Fig. 9. MIX (a) and HEA (b) melts phases structure and composition (at. %)

Рис. 9. Структура и состав (ат. %) фаз расплавов MIX (a) и ВЭС (b)

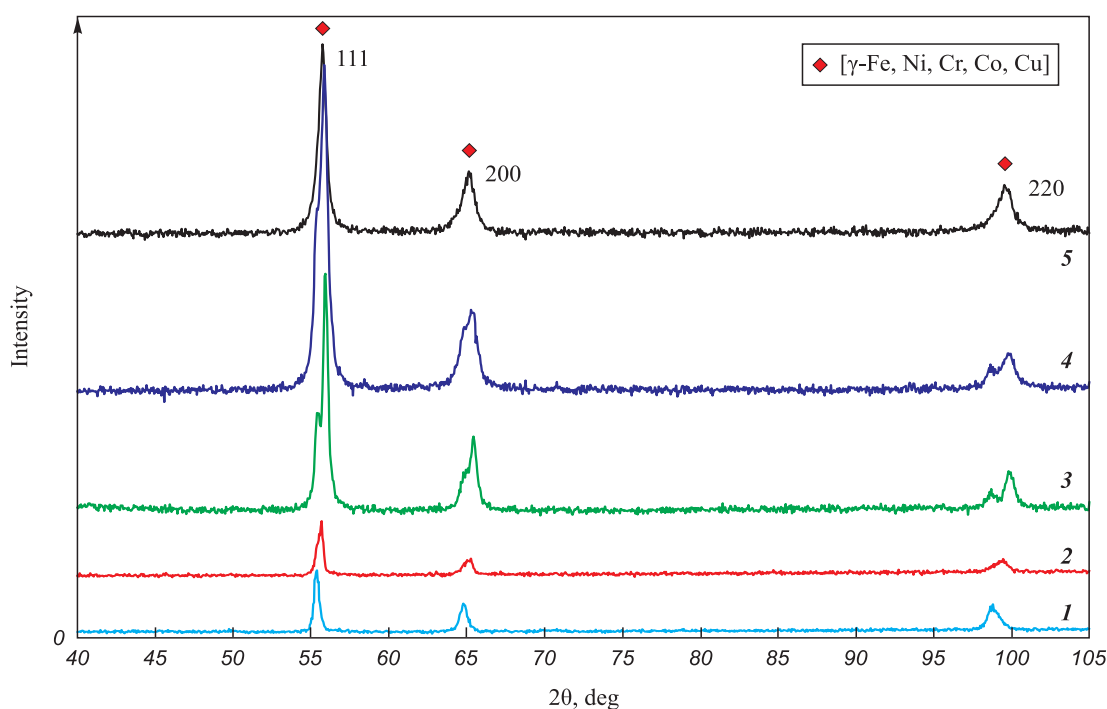


Fig. 10. SPS method melting and sintering products X-ray patterns
1 – HEA melt, 2 – MIX melt, 3 – HEA SPS (800 °C), 4 – HEA SPS (900 °C), 5 – HEA SPS (1000 °C)

Рис. 10. Рентгенограммы продуктов плавления и спекания методом ИПС
1 – расплав ВЭС, 2 – расплав MIX, 3 – ВЭС ИПС (800 °C), 4 – ВЭС ИПС (900 °C), 5 – ВЭС ИПС (1000 °C)

is a 5-component phase with the averaged formula $\text{Cu}_{1.2}\text{Fe}_{1.4}\text{Ni}_{1.4}\text{Co}_{1.4}\text{Cr}$ with small additions of the above 5-, 4- and 3-component phases.

The microhardness of samples MIX and HEA without carbide grains is in the range of 2.4–6.9 GPa. Its

minimum value corresponds to areas with high copper content, maximum – with high chromium concentration. Microhardness of MIX and HEA samples with 30–70 % Ti + C in the initial mixture is 3.6–10.0 GPa and partially depends on copper and chrome concentra-

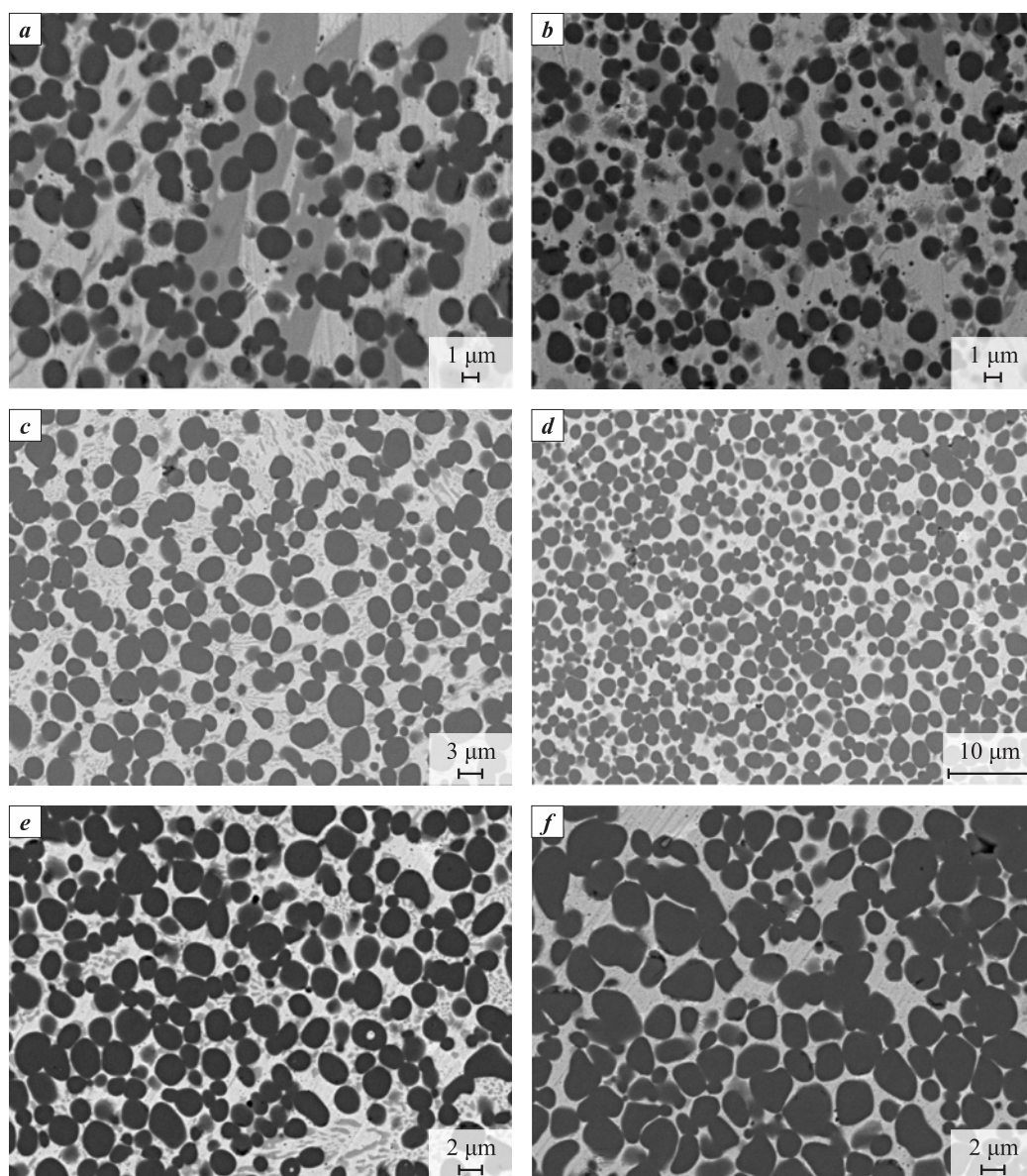


Fig. 11. The alloys microstructure after melt crystallization
a – 30(Ti + C) + 70MIX; *b* – 30(Ti + C) + 70HEA; *c* – 40(Ti + C) + 60MIX;
d – 40(Ti + C) + 60HEA; *e* – 60(Ti + C) + 40MIX; *f* – 70(Ti + C) + 30MIX

Рис. 11. Микроструктура сплавов после кристаллизации расплава
a – 30(Ti + C) + 70MIX; *b* – 30(Ti + C) + 70ВЭС; *c* – 40(Ti + C) + 60MIX;
d – 40(Ti + C) + 60ВЭС; *e* – 60(Ti + C) + 40MIX; *f* – 70(Ti + C) + 30MIX

tion, but the main contribution to microhardness values is made by the TiC particles closeness to each other and their even distribution throughout the cermet volume. The TiC particles microhardness is 25–35 GPa and corresponds to the known data [25].

Conclusion

The possibility of obtaining cermets with a high-entropic binder by using a mixture of titanium and carbon forming TiC particles as an energy additive was shown. This makes it possible to reduce the cer-

Table 2. Alloys TiC particles volume concentration

Таблица 2. Объемная концентрация частиц TiC в сплавах

No.	Composition	$N, 10^3 \text{ mm}^{-3}$
1	30(Ti + C) + 70HEA	200
2	40(Ti + C) + 60HEA	112
3	30(Ti + C) + 70MIX	117
4	40(Ti + C) + 60MIX	37
5	60(Ti + C) + 40MIX	54
6	70(Ti + C) + 30MIX	105

met production energy costs by carrying out the process in combustion or thermal explosion mode. At the initial temperature of 500 °C, the combustion limit of the samples comes at the Ti + C concentration less than 30 %. During the cermet synthesis the high-entropic alloy FeNiCoCrCu binder splits into several phases, but the basis of the alloy is formed by a 5-component phase with the averaged formula $\text{Cu}_{1.2}\text{Fe}_{1.4}\text{Ni}_{1.4}\text{Co}_{1.4}\text{Cr}$.

Preliminary HEA production by mechanical alloying is not a necessary stage of initial powders preparation process, since the high-entropic binder is formed from a mixture of initial metals during the high-temperature cermet synthesis. The number of TiC particles in the volume unit in cermet with a binder from a pre-prepared HEA is 1.5–3.0 times higher than in an alloy with a binder from a mixture of metals.

References / Список литературы

1. Yeh J.-W., Chen S.-K., Lin S.-J., Gan J.-Y., Chin T.-S., Shun T.-T., Tsau C.-H., Chang S.-Y. Nanostructured high-entropy alloys with multiple principal elements: novel alloy design concepts and outcomes. *Advanced Engineering Materials*. 2004;6(5):299–303. <https://doi.org/10.1002/adem.200300567>
2. Cantor B., Chang I.T.H., Knight P., Vincent A.J.B. Microstructural development in equiatomic multicomponent alloys. *Materials Science and Engineering: A*. 2004;375–377: 213–218. <https://doi.org/10.1016/j.msea.2003.10.257>
3. Gludovatz B., Hohenwarter A., Catoor D., Chang E.H., George E.P., Ritchie R.O. A fracture-resistant high-entropy alloy for cryogenic applications. *Science*. 2014;345(6201): 1153–1158. <https://doi.org/10.1126/science.1254581>
4. Lee C.P., Chen Y.Y., Hsu C.Y., Yeh J.W., Shih H.C. The effect of boron on the corrosion resistance of the high entropy alloys $\text{Al}_{0.5}\text{CoCrCuFeNiB}_x$. *Journal of the Electrochemical Society*. 2007;154(8):424–430. <https://doi.org/10.1149/1.2744133>
5. Shkodich N.F., Kuskov K.V., Sedegov A.S., Kovalev I.D., Panteleeva A.V., Vergunova Yu.S., Scheck Yu.B., Panina E., Stepanov N., Serhiienko I., Moskovskikh D. Refractory TaTiNb, TaTiNbZr, and TaTiNbZrX (X = Mo, W) high entropy alloys by combined use of high energy ball milling and spark plasma sintering: Structural characterization, mechanical properties, electrical resistivity, and thermal conductivity. *Journal of Alloys and Compounds*. 2022;893:162030. <https://doi.org/10.1016/j.jallcom.2021.162030>
6. Zuo T.T., Gao M.C., Ouyang L.Z., Yang X., Cheng Y.Q., Feng R., Chen S.Y., Liaw P. K., Hawk J.A., Zhang Y. Tailoring magnetic behavior of CoFeMnNiX (X = Al, Cr, Ga, and Sn) high entropy alloys by metal doping. *Acta Materialia*. 2017;130:10–18. <https://doi.org/10.1016/j.actamat.2017.03.013>
7. Tsai M.-H., Yeh J.-W. High-entropy alloys: A critical review. *Materials Research Letters*. 2014;2(3):107–123. <https://doi.org/10.1080/21663831.2014.912690>
8. Ye Y.F., Wang Q., Lu J., Liu C.T., Yang Y. High-entropy alloy: challenges and prospects. *Materials Today*. 2016;19(6):349–362. <https://doi.org/10.1016/j.mattod.2015.11.026>
9. Miracle D.B., Senkov O.N. A critical review of high entropy alloys and related concepts. *Acta Materialia*. 2017;122: 448–511. <https://doi.org/10.1016/j.actamat.2016.08.081>
10. Velo I.L., Gotor F.J., Alcalá M.D., Real C., Córdoba J.M. Fabrication and characterization of WC-HEA cemented carbide based on the CoCrFeNiMn high entropy alloy. *Journal of Alloys and Compounds*. 2018;746:1–8. <https://doi.org/10.1016/j.jallcom.2018.02.292>
11. Rogal L., Kalita D., Tarasek A., Bobrowski P., Czerwinski F. Effect of SiC nano-particles on microstructure and mechanical properties of the CoCrFeMnNi high entropy alloy. *Journal of Alloys and Compounds*. 2017;708:344–352. <https://doi.org/10.1016/j.jallcom.2017.02.274>
12. Fan Q.C., Li B.S., Zhang Y. The microstructure and properties of $(\text{FeCrNiCo})\text{Al}_x\text{Cu}_y$ high-entropy alloys and their TiC-reinforced composites. *Materials Science and Engineering: A*. 2014;598:244–250. <https://doi.org/10.1016/j.msea.2014.01.044>
13. Jiang P.F., Zhang C.H., Zhang S., Zhang J.B., Chen J., Liu Y. Fabrication and wear behavior of TiC reinforced FeCoCrAlCu-based high entropy alloy coatings by laser surface alloying. *Materials Chemistry and Physics*. 2020;255:123571. <https://doi.org/10.1016/j.matchemphys.2020.123571>
14. Cai Y., Zhu L., Cui Y., Shan M., Li H., Xin Y., Han J. Fracture and wear mechanisms of FeMnCrNiCo + x(TiC) composite high-entropy alloy cladding layers. *Applied Surface Science*. 2021;543:148794. <https://doi.org/10.1016/j.apsusc.2020.148794>
15. Zhu G., Liu Y., Ye J. Fabrication and properties of Ti(C,N)-based cermets with multi-component AlCoCrFeNi high-entropy alloys binder. *Materials Letters*. 2013;113:80–82. <https://doi.org/10.1016/j.matlet.2013.08.087>
16. Wang Z., Xiong J., Guo Z., Yang T., Liu J., Chai B. The microstructure and properties of novel Ti(C,N)-based cermets with multi-component CoCrFeNiCu high-entropy alloy binders. *Materials Science and Engineering: A*. 2019;766:138345. <https://doi.org/10.1016/j.msea.2019.138345>
17. De la Oña A.G., Sayagués M.J., Chicardi E., Gotor F.J. Development of Ti(C,N)-based cermets with (Co,Fe,Ni)-based high entropy alloys as binder phase. *Journal of Alloys and Compounds*. 2020;814:152218. <https://doi.org/10.1016/j.jallcom.2019.152218>
18. Yang S., Xiong J., Guo Z., Wu B., Yang T., You Q., Liu J., Deng C., Fang D., Gou S., Yu Z., Chend S. Effects of CrMnFeCoNi additions on microstructure, mechanical properties and wear resistance of Ti(C,N)-based cermets. *Journal of Materials Research and Technology*. 2022;17: 2480–2494. <https://doi.org/10.1016/j.jmrt.2022.02.021>
19. Rogachev A.S., Vadchenko S.G., Kochetov N.A., Kovalev D.Yu., Kovalev I.D., Shchukin A.S., Gryadunov A.N., Baras F., Politano O. Combustion synthesis of TiC-based ceramic-metal composites with high entropy alloy binder. *Journal of the European Ceramic Society*. 2020;40(7):2527–2532. <https://doi.org/10.1016/j.jeurceramsoc.2019.11.059>

20. Shkodich N.F., Kovalev I.D., Kuskov K.V., Kovalev D.Yu., Vergunova Yu.S., Scheck Yu.B., Vadchenko S.G., Politano O., Baras F., Rogachev A.S. Fast mechanical synthesis, structure evolution, and thermal stability of nanostructured CoCrFeNiCu high entropy alloy. *Journal of Alloys and Compounds*. 2022;893:161839. <https://doi.org/10.1016/j.jallcom.2021.161839>
21. Vadchenko S.G., Boyarchenko O.D., Shkodich N.F., Rogachev A.S. Thermal explosion in various Ni–Al systems: Effect of mechanical activation. *International Journal of Self-Propagating High-Temperature Synthesis*. 2013;22(1):60–64. <https://doi.org/10.3103/S1061386213010123>
22. Inyukhin M.V., Korzhavnyi A.P., Prasitskii G.V. Parameters and techniques of receiving of heat-absorbent materials for semiconductor device. *Naukoemkie tekhnologii*. 2014;15(2):10–19. (In Russ.).
Инюхин М.В., Коржавый А.П., Прасицкий Г.В. Параметры и техника получения теплоотводящих материалов для полупроводниковых приборов. *Научные технологии*. 2014;15(2):10–19.
23. Shirasawa N., Takigawa Y., Uesugi T., Higashi K. Calculation of alloying effect on formation enthalpy of TiCu intermetallics from first-principles calculations for designing Ti–Cu-system metallic glasses. *Philosophical Magazine Letters*. 2016;96(1):27–34. <https://doi.org/10.1080/09500839.2015.1134833>
24. Grinchuk P.S., Rabinovich O.S. Percolation phase transition in combustion of heterogeneous mixtures. *Combustion, Explosion and Shock Waves*. 2004;40(4):408–418. <https://doi.org/10.1023/B:CESW.0000033563.66432.1c>
Гринчук П.С., Рабинович О.С. Перколяционный фазовый переход при горении гетерогенных смесей. *Физика горения и взрыва*. 2004;40(4):41–53.
25. Carbide, nitride, and boride materials synthesis and processing. Ed. A.W. Weimer. London: Publ. Chapman & Hall, 1997. 671 p.

Information about the Authors



Sergei G. Vadchenko – Cand. Sci. (Phys.-Math.), Leading Researcher, Laboratory of dynamics of microheterogeneous processes, Merzhanov Institute of Structural Macrokinetics and Materials Science of the Russian Academy of Sciences (ISMAN)

ORCID: 0000-0002-2360-2114

E-mail: vadchenko@ism.ac.ru

Yulia S. Vergunova – Postgraduate Student, Laboratory of dynamics of microheterogeneous processes of ISMAN

ORCID: 0000-0002-9805-2575

E-mail: yulya-ser94@yandex.ru

Aleksander S. Rogachev – Dr. Sci. (Phys.-Math.), Prof., Head of the Laboratory of dynamics of microheterogeneous processes of ISMAN

ORCID: 0000-0003-1554-0803

E-mail: rogachev@ism.ac.ru

Ivan D. Kovalev – Cand. Sci. (Phys.-Math.), Senior Researcher, Laboratory of X-ray investigation of ISMAN

ORCID: 0000-0003-4710-837X

E-mail: i2212@yandex.ru

Nina I. Mukhina – Technologist, Laboratory of materials science of ISMAN

ORCID: 0000-0002-5089-0908

E-mail: muxinanina2012@yandex.ru

Сведения об авторах

Сергей Георгиевич Вадченко – к.ф.-м.н., вед. науч. сотрудник лаборатории динамики микрогетерогенных процессов, Институт структурной макрокинетики и проблем материаловедения им. А.Г. Мерджанова РАН (ИСМАН)

ORCID: 0000-0002-2360-2114

E-mail: vadchenko@ism.ac.ru

Юлия Сергеевна Вергунова – аспирант лаборатории динамики микрогетерогенных процессов, ИСМАН

ORCID: 0000-0002-9805-2575

E-mail: yulya-ser94@yandex.ru

Александр Сергеевич Рогачев – д.ф.-м.н., проф., заведующий лабораторией динамики микрогетерогенных процессов, ИСМАН

ORCID: 0000-0003-1554-0803

E-mail: rogachev@ism.ac.ru

Иван Дмитриевич Ковалев – к.ф.-м.н., ст. науч. сотрудник лаборатории рентгеноструктурных исследований, ИСМАН

ORCID: 0000-0003-4710-837X

E-mail: i2212@yandex.ru

Нина Илларионовна Мухина – технолог лаборатории физического материаловедения, ИСМАН

ORCID: 0000-0002-5089-0908

E-mail: muxinanina2012@yandex.ru

Contribution of the Authors



S. G. Vadchenko – setting the goal and objectives of the study, preparing the text, formulating conclusions.

Yu. S. Vergunova – preparation and conduct of the experiment, management of the experiment.

A. S. Rogachev – scientific guidance, the formation of the main concept, text correction, correction of conclusions.

I. D. Kovalev – X-ray phase analysis.

N. I. Mukhina – sample preparation and SEM.

Вклад авторов

С. Г. Вадченко – постановка цели и задачи исследования, подготовка текста, формулировка выводов.

Ю. С. Вергунова – подготовка и проведение эксперимента, руководство проведением эксперимента.

А. С. Рогачев – научное руководство, формирование основной концепции, корректировка текста, корректировка выводов.

И. Д. Ковалев – проведение рентгенофазового анализа.

Н. И. Мухина – подготовка образцов и СЭМ.

Received 19.04.2022

Revised 23.05.2022

Accepted 25.05.2022

Статья поступила 19.04.2022 г.

Доработана 23.05.2022 г.

Принята к публикации 25.05.2022 г.